Power Electronic Systems
Laboratory

Proceedings of the 14th IEEE Workshop on Control and Modeling for Power Electronics (COMPEL 2013), Salt Lake City, USA, June 23-26, 2013

Practical Characterization of EMI Filters Replacing CISPR 17 Approximate Worst Case Measurements

I. Kovacevic,
F. Krismer,
S. Schroth,
J. W. Kolar

Eidgenössische Technische Hochschule Zürich
Swiss Federal Institute of Technology Zurich

Practical Characterization of EMI Filters Replacing CISPR 17 Approximate Worst Case Measurements

I. Kovačević, F. Krismer, S. Schroth, and J. W. Kolar
Power Electronic Systems Laboratory,
ETH Zurich,
Switzerland
E-mail: kovacevic@lem.ee.ethz.ch

***Abstract*—A common approach for selecting a suitable EMI filter is detailed based on the example of a realized single-phase 500 W PFC rectifier. The presented work separates conducted EMI noise into Differential Mode (DM) and Common Mode (CM) components and derives expressions for the DM and CM insertion losses achieved if a given EMI filter is connected to a dedicated power converter. With the use of hardware measurement results it is shown that the impedances of the EMI filter and the PFC rectifier have a considerable impact on the realized insertion losses, which, at particular frequencies, may be even less than approximate worst-case estimations proposed in CISPR 17.**

NOMENCLATURE

f	frequency,
$\omega = 2\pi f$	angular frequency,
$\underline{V}_{\mathrm{pk}}(\mathrm{j}\omega)$	complex magnitude of the spectral component at ω,
$\underline{V}(\mathrm{j}\omega) = \dfrac{\underline{V}_{\mathrm{pk}}(\mathrm{j}\omega)}{\sqrt{2}}$	complex RMS value,
$V(\mathrm{j}\omega) = \lvert\underline{V}(\mathrm{j}\omega)\rvert$	absolute value of $\underline{V}(\mathrm{j}\omega)$,
$\arg[\underline{V}(\mathrm{j}\omega)]$	phase angle of $\underline{V}(\mathrm{j}\omega)$;
$\underline{V}_{\mathrm{s,DM}}$, $\underline{V}_{\mathrm{s,CM}}$	diff. mode (DM) and common mode (CM) noise source voltages,
$\underline{V}_{\mathrm{f,DM}}$, $\underline{V}_{\mathrm{f,CM}}$	input voltages applied to the EMI filter (DM and CM),
$\underline{V}_{\mathrm{DM}}$, $\underline{V}_{\mathrm{CM}}$	filter output voltages;
$\underline{Z}_{\mathrm{s}}$, $\underline{Z}_{\mathrm{o}}$	source and load impedances,
IL_{50}	insertion loss for $\underline{Z}_{\mathrm{s}} = \underline{Z}_{\mathrm{o}} = 50\,\Omega$,
$IL_{\underline{Z}_{\mathrm{s}}/\underline{Z}_{\mathrm{o}}}$	insertion loss for dedicated $\underline{Z}_{\mathrm{s}}$ and $\underline{Z}_{\mathrm{o}}$, e.g. $IL_{0.1/100}$ is the insertion loss for $\underline{Z}_{\mathrm{s}} = 0.1\,\Omega$ and $\underline{Z}_{\mathrm{o}} = 100\,\Omega$,
$(IL)_{\mathrm{dB}}$	insertion loss expressed in decibel, $(IL)_{\mathrm{dB}} = 20\,\mathrm{dB} \cdot \log_{10}(IL)$.

(N.B.: This list summarizes only the most important symbols.)

I. INTRODUCTION

EMI input filters have to be used as the interface between power converters and the mains in order to ensure Electromagnetic Compatibility (EMC) of power electronic systems connected to the AC power lines. A prominent example is the single-phase Power Factor Correction (PFC) boost rectifier with Electromagnetic Interference (EMI) input filter, depicted in **Fig. 1**, which is used as an illustrative example throughout this Paper.

The EMC standards defined by international institutions, such as the European CISPR, include the standardization of EMC measurement methods and specifications of internationally accepted limits of EMI noise levels. For industrial, scientific, and medical equipment the CISPR 11 standard [1] is applicable, which limits conducted EMI emissions based on maximum allowable scaled average absolute and quasi-peak voltages, in the frequency range between $150\,\mathrm{kHz}$ and $30\,\mathrm{MHz}$.[1] Thus, a design engineer determines the EMI noise generated without EMI filter and considers an EMI filter that realizes the required voltage attenuation. A suitable EMI filter may be obtained based on a dedicated design procedure, e.g. according to [4], [5], or, more commonly, by selecting a commercial EMI filter. Manufacturers of EMI filters, however, typically specify insertion losses of EMI filters for source and load resistances of $50\,\Omega$. In this context, the use of a $50\,\Omega$ load resistor may be defended on the basis of mains impedance measurements, e.g. presented in [7], [8], which suggest a $50\,\Omega$ resistor to represent a rough approximation of an average mains impedance at frequencies between $150\,\mathrm{kHz}$ and $30\,\mathrm{MHz}$. The inner impedance of a power converter, however, cannot be replaced by a $50\,\Omega$ resistor at all.

Initial proposals related to an improved characterization of EMI filter attenuation suggest insertion loss measurements to be conducted with a source resistance of $0.1\,\Omega$ and a load resistance of $100\,\Omega$ and vice versa, which is identified as worst-case condition in [9] and referred to as approximate worst-case method in [10]. In fact, a detailed inspection reveals that resonance effects at the filter ports (PFC rectifier $\leftrightarrow$ EMI filter and EMI filter $\leftrightarrow$ mains) may further deteriorate the actual insertion loss at particular frequencies. Related analytical investigations, including the concept of impedance domains and worst-case solutions for particular assumptions (e.g. particular conditions for source and/or load impedances), are detailed in [11], [12].

[1] The measurement equipment used to determine average absolute and quasi-peak voltages is specified in CISPR 16 [2]. Both, average absolute and quasi-peak voltages, are scaled such that the test receiver returns the RMS value in case of a purely sinusoidal input signal, i.e. the overall DC gain is $1/\sqrt{2}$ [3].

978-1-4673-4916-1/13/$31.00 ©2013 IEEE

The IEEE Standard 1560-2005 [13] counteracts the unsatisfactory status of having very limited possibilities to predict the actually achieved filter attenuation by including additional measurement methods with source and load impedances different to $50\,\Omega$ (in addition to those of [10]). This extends the set of potentially achieved insertion losses. Still, a filter, which is solely selected based on attenuation or insertion loss curves without taking the filter impedance and the actually present converter impedance into account, may be overdimensioned and / or may fail to sufficiently attenuate EMI noise, due to resonance effects at particular frequencies.

Accurate methods capable of modeling the impacts of source and load impedances on the achieved insertion losses are based on a full characterization of the EMI filter, e.g. using scattering parameters, which, in addition to differential mode (DM) and common mode (CM) attenuations, also consider mode conversions (DM to CM and CM to DM) [13]–[15]. These descriptions, however, require high numbers of complex and frequency dependent parameters and are well suited for electric circuit simulation but of less practical value. In practice, differential mode (DM) and common mode (CM) are often treated separately, which features reduced system complexity and improved technical insight; a certain error due to unbalanced filter component values, cf. [16], is accepted.

A prediction of DM and CM insertion losses achieved for particular source and load impedances is feasible with the findings of [11], [17], [18]. The analytical findings presented in these publications are derived based on a filter description with four A-parameters (cascade parameters), which need to be determined for DM and CM, separately. Still, approximations of expected insertion losses with reduced numbers of required parameters are feasible; different approximations are presented in [17], [18]. Due to the chosen theoretical approach based on quadrupole parameters, however, it is difficult to gain a deeper understanding of the technical context at hand.

This paper presents a procedure for predicting the actually realized insertion loss of an EMI filter. The presented method requires the DM and CM filter impedances at the interface between PFC rectifier and EMI filter and the DM and CM converter impedances in addition to already available $50\,\Omega$ insertion loss curves. In this context, the measurement setup used to determine conducted noise and the definitions of DM and CM are revisited in **Section II** and a common procedure used to select an EMI filter is outlined in **Section III**. **Section IV** investigates how source and load impedances influence the insertion losses. Based on experimental results obtained from an example PFC rectifier the implications of filter and converter impedances on the insertion losses are discussed in **Section V**.

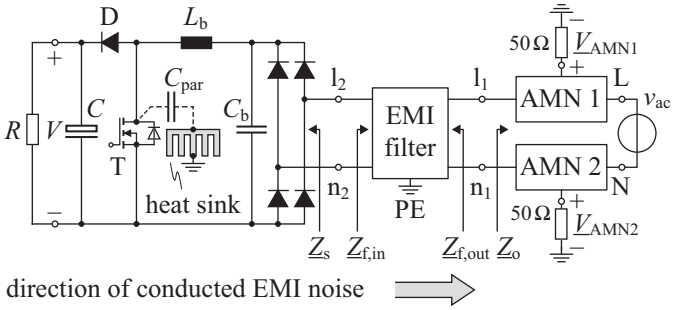

Fig. 1: Setup for measuring the conducted EMI noise generated by a boost-type PFC rectifier. The boost-type PFC rectifier is drawn with the DC port at the left side and the AC port at the right side in order to focus on the noise propagation path and to maintain consistency with the equivalent noise source models depicted in Fig. 5. The emitted EMI noise is measured at the measurement ports of the Artificial Mains Networks (AMNs, Fig. 2), which provide the output voltages $\underline{V}_{AMN1,2}$. The depicted impedances at the filter ports are different for differential mode (DM) and common mode (CM) excitations, cf. Fig. 5. Furthermore, the depicted parasitic capacitance, C_{par}, which is mostly formed by the back side of the MOSFET, thermal interface pad, and the earthed heat sink, provides the main current path for common mode EMI noise [6].

II. Measuring and Modeling Conducted EMI Noise

The boost-type PFC rectifier of Fig. 1, which serves as an example application, is specified in the list below.

- Mains voltage amplitude: $V_{ac,pk} = 325\,\mathrm{V}$.
- Mains frequency: $f_{ac} = 50\,\mathrm{Hz}$.
- Nominal output power: $P = 500\,\mathrm{W}$.
- Nominal output voltage: $V = 400\,\mathrm{V}$.
- Switching frequency: $f_s = 500\,\mathrm{kHz}$.

A. Measurement of conducted EMI noise

The commonly used method to determine conducted EMI emissions generated by power electronic converters is shown in Fig. 1 for a single phase PFC rectifier. There, Line Impedance Stabilization Networks or Artifical Mains Networks (AMNs, **Fig. 2**) are inserted between the mains and the PFC rectifier's EMI filter. Each AMN provides a port for voltage measurement, i.e. $\underline{V}_{AMN}(\mathrm{j}\omega)$ in **Fig. 3**. The voltage at that port must comply with the limits defined in the considered regulations, e.g. CISPR 11.[2] The AMN, in

[2]The $50\,\Omega$ resistor depicted in Fig. 1 denotes the $50\,\Omega$ input impedance of the test receiver. A dedicated $50\,\Omega$ resistor needs to be used if no test receiver is currently connected to the measurement port of the AMN. Further details on EMI measurements are given in [2].

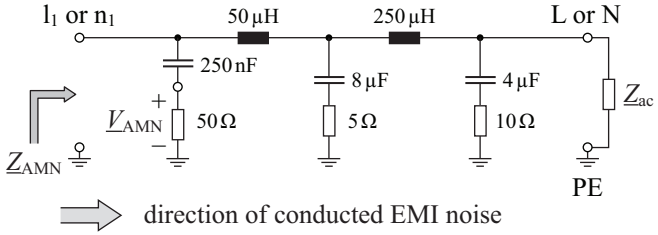

Fig. 2: Circuit of the AMN (from [2]). The l_1-n_1-ports are connected to the device under test and the l_2-n_2-ports are connected to the mains. In the considered frequency range, $150\,\mathrm{kHz} < f < 30\,\mathrm{MHz}$, the $250\,\mathrm{nF}$ capacitor and the $50\,\mu\mathrm{H}$ inductor at the input side redirect the EMI noise to the $50\,\Omega$ input resistance of the test receiver, marked with $\underline{V}_{AMN}$. $\underline{Z}_{ac}$ denotes the mains impedance.

addition, realizes an impedance at its input port ($\underline{Z}_{\mathrm{AMN}}$), which is nearly independent of the actual mains impedance, $\underline{Z}_{\mathrm{ac}}$, for frequencies greater than approximately 20 kHz, cf. Fig. 3. Thus, the use of AMNs allows for reproducible measurements.

The AMN of Fig. 3 is parameterized according to [2] and yields $\underline{Z}_{\mathrm{AMN}} \approx 50\,\Omega$ in the frequency range considered for conducted EMI, $150\,\mathrm{kHz} < f < 30\,\mathrm{MHz}$. Thus, $\underline{Z}_{\mathrm{AMN}}$ can be approximately replaced by a $50\,\Omega$ resistor (Fig. 3), which is used to simplify the subsequent analysis.

B. Differential Mode (DM) and Common Mode (CM) noise

The EMI noise generated by a power electronic converter is commonly separated into DM and CM noise, e.g. in [5], due to essentially different filter components and filter structures required. **Fig. 4** illustrates the formation of DM and CM noise at the measurement ports of the AMNs in the considered frequency range, $f > 150\,\mathrm{kHz}$. The Device Under Test (DUT), i.e. PFC rectifier plus EMI filter, generates high frequency EMI noise and the AMNs redirect this noise to the respective $50\,\Omega$ measurement resistors.

The currents through the two $50\,\Omega$ resistors of Fig. 4 can be separated into DM currents (blue path, no earth current involved) and CM currents (red path, forms the earth current),

$$\underline{I}_{\mathrm{l}} = \underline{I}_{\mathrm{CM}} + \underline{I}_{\mathrm{DM}}, \quad \underline{I}_{\mathrm{n}} = \underline{I}_{\mathrm{CM}} - \underline{I}_{\mathrm{DM}}, \tag{1}$$

which results in:

$$\underline{I}_{\mathrm{DM}} = \frac{\underline{I}_{\mathrm{l}} - \underline{I}_{\mathrm{n}}}{2}, \quad \underline{I}_{\mathrm{CM}} = \frac{\underline{I}_{\mathrm{l}} + \underline{I}_{\mathrm{n}}}{2}. \tag{2}$$

Accordingly, the measured voltages $\underline{V}_{\mathrm{AMN1}}$ and $\underline{V}_{\mathrm{AMN2}}$ can be converted into the DM and CM noise voltages:[3]

$$\underline{V}_{\mathrm{DM}} = \underline{I}_{\mathrm{DM}}\,50\,\Omega = \frac{\underline{V}_{\mathrm{AMN1}} - \underline{V}_{\mathrm{AMN2}}}{2}, \tag{3}$$

$$\underline{V}_{\mathrm{CM}} = \underline{I}_{\mathrm{CM}}\,50\,\Omega = \frac{\underline{V}_{\mathrm{AMN1}} + \underline{V}_{\mathrm{AMN2}}}{2}. \tag{4}$$

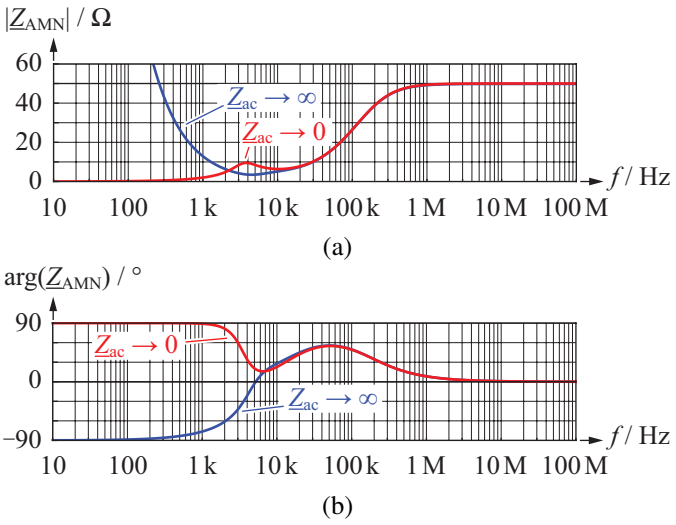

Fig. 3: Input impedance of the AMN for $\underline{Z}_{\mathrm{ac}} \to \infty$ (blue) and $\underline{Z}_{\mathrm{ac}} \to 0$ (red): (a) absolute value, (b) phase angle. It can be seen that $\underline{Z}_{\mathrm{AMN}}$ is independent of the mains impedance for frequencies greater than 20 kHz, which corresponds to the results depicted in Fig. 6 in [19].

C. Modeling the source of conducted EMI emissions

In the given example, i.e. the PFC rectifier depicted in Fig. 1, the continuously repeated switching of the semiconductor switch T is the source of the EMI noise generated. Simple equivalent circuits for modeling the investigated PFC rectifier regarding generation of conducted EMI noise (DM and CM) are presented in [4], [6]. In each model the semiconductor switch is replaced by a rectangular voltage source with an inner

[3] Different definitions of the DM voltage are found in literature, e.g. [5], [16], [20], [21]; either (3) or $\underline{V}_{\mathrm{DM}} = \underline{V}_{\mathrm{AMN1}} - \underline{V}_{\mathrm{AMN2}}$ is used. With (3) and (4) the obtained DM and CM voltages are directly the output voltages of the DM / CM separator circuits proposed in [20], [21].

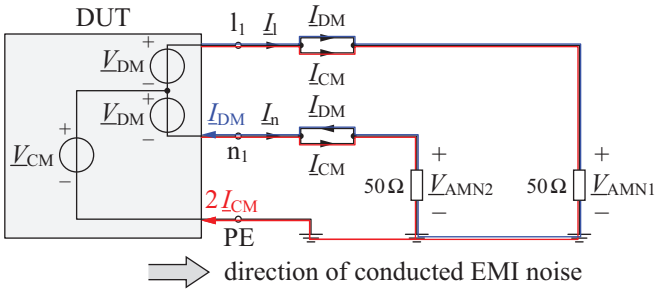

Fig. 4: Proposed separation of the phase currents $\underline{I}_{\mathrm{l}}$ and $\underline{I}_{\mathrm{n}}$ into the DM and CM currents $\underline{I}_{\mathrm{DM}}$ and $\underline{I}_{\mathrm{CM}}$, respectively. This approach yields differential and common mode voltages according to (3), (4) [16], [20].

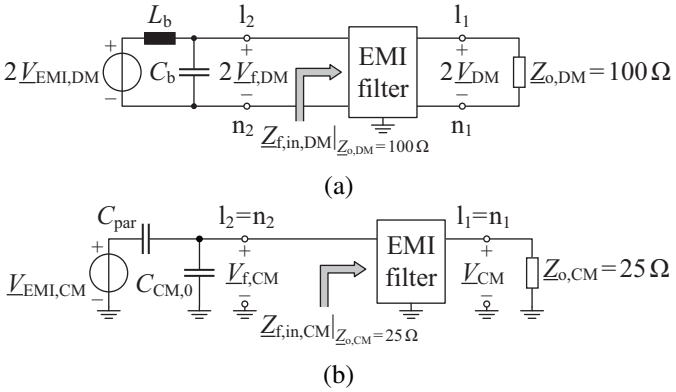

Fig. 5: Simplified equivalent circuits for modeling sources and impedance networks relevant for conducted EMI noise: (a) DM [4]; (b) CM [6]. The DM model considers the impedances of the boost inductor L_{b} and the filter capacitor C_{b}. The CM model employs the two capacitors C_{par} and $C_{\mathrm{CM,0}}$, which are obtained according to [6].

impedance. According to [4], [6], the spectra of the voltage sources (magnitude values) can be approximated with

$$2V_{\text{EMI,DM,pk}}(nf_\text{s}) = V_{\text{EMI,CM,pk}}(nf_\text{s}) \approx \frac{1}{n}\sqrt{\frac{4}{\pi}V_{\text{ac,pk}}V_0 - V_{\text{ac,pk}}^2} \quad \forall \quad n \in \mathbb{N}. \tag{5}$$

Fig. 5(a) depicts the considered DM model of the noise source to the left of the l_2-n_2-port, i.e. the DM noise voltage and a filter network formed with L_b and C_b [4].[4] The CM model shown in **Fig. 5(b)** contains the CM noise voltage and a capacitor network [6]. By applying Thévenin's theorem, equivalent voltage sources with series connected inner impedances can be derived for DM and CM, respectively:[5]

$$\underline{2V}_{\text{s,DM}} = \frac{2V_{\text{EMI,DM,pk}}}{\sqrt{2}}\frac{\underline{Z}_{C_\text{b}}}{\underline{Z}_{L_\text{b}} + \underline{Z}_{C_\text{b}}} \text{ with } \underline{Z}_{\text{s,DM}} = \underline{Z}_{L_\text{b}} || \underline{Z}_{C_\text{b}}, \tag{6}$$

$$\underline{V}_{\text{s,CM}} = \frac{V_{\text{EMI,CM,pk}}}{\sqrt{2}}\frac{\underline{Z}_{C_{\text{CM,0}}}}{\underline{Z}_{C_\text{par}} + \underline{Z}_{C_{\text{CM,0}}}} \text{ with}$$

$$\underline{Z}_{\text{s,CM}} = \underline{Z}_{C_\text{par}} || \underline{Z}_{C_{\text{CM,0}}}. \tag{7}$$

Moreover, different termination impedances are effective for the EMI filter in case of DM and CM. The effective termination impedance for DM, $\underline{Z}_{\text{o,DM}}$, is $100\,\Omega$, since $\underline{I}_\text{DM}$ is passed through two $50\,\Omega$ resistors in series, cf. Fig. 4. As a consequence and due to (3) a factor 2 needs to be considered for the DM voltages in order to correctly consider the actual level of conducted EMI noise at each phase. For CM the effective termination impedance, $\underline{Z}_{\text{o,CM}}$, is $25\,\Omega$, due to identical CM potentials of l_1 and n_1. Thus, the actual CM voltage, $\underline{V}_\text{CM}$, is directly applied to this effective impedance.

The presented noise model is simple, however, only limited accuracy is expected. Improved accuracy may be achieved with more advanced noise models, e.g. the model proposed in [22].

D. Insertion loss of an EMI filter

The insertion loss, typically determined according to **Fig. 6** with a generator with $50\,\Omega$ source impedance and a test receiver with $50\,\Omega$ measurement resistance, denotes the absolute value of the ratio of the output voltages obtained without and with filter employed [e.g. $\underline{V}'_\text{DM}(f)$ and $\underline{V}_\text{DM}(f)$ in Fig. 6(a) and (b), respectively], cf. [17]. In case of $50\,\Omega$ source and load impedances the insertion loss is equal to

$$IL_{\text{50,DM}}(f) = \left|\frac{2\underline{V}'_\text{DM}(f)}{2\underline{V}_\text{DM}(f)}\right| = \left|\frac{\underline{V}_\text{g}/2}{2\underline{V}_\text{DM}(f)}\right| \tag{8}$$

for DM and

$$IL_{\text{50,CM}}(f) = \left|\frac{\underline{V}_\text{g}/2}{\underline{V}_\text{CM}(f)}\right| \tag{9}$$

for CM.

III. Common approach for selecting an EMI filter

In a first step the emitted EMI noise is measured without filter, e.g. as suggested in [5]. Based on the measurement results and the allowable DM and CM voltages the required insertion losses of the filter are determined and a suitable filter can be designed or selected.

The voltage measured at one test receiver is equal to the superposition of $\underline{V}_\text{CM}$ and $\underline{V}_\text{DM}$. Thus, the maximum measurement voltages are:

- $\max(V_\text{AMN1}) = V_\text{CM} + V_\text{DM}$ applies for $\arg(\underline{V}_\text{DM}) = \arg(\underline{V}_\text{CM})$,
- $\max(V_\text{AMN2}) = V_\text{CM} + V_\text{DM}$ applies for $\arg(\underline{V}_\text{DM}) = \arg(\underline{V}_\text{CM}) + 180°$.

Since measurement results on insertion losses already available in filter data sheets only include absolute values of the insertion losses and no information on the introduced phase shifts, the actual EMI noise is estimated according to:

$$V_{\text{AMN1,2}}(f) \leq V_\text{DM}(f) + V_\text{CM}(f) < V_\text{CISPR}(f) \tag{10}$$

($V_\text{DM} + V_\text{CM}$ is the estimated EMI noise, and V_CISPR is the allowed noise level). With (10) the EMI noise may be slightly overestimated, which, however, is considered to be acceptable, since unmodeled effects, e.g. mode conversion, may increase the total EMI noise again.

The design or selection of a suitable EMI filter is based on a measurement of the conducted EMI noise generated by the PFC rectifier of Fig. 1 *without* EMI filter being used, cf. [5]. This measurement requires the measured EMI noise levels

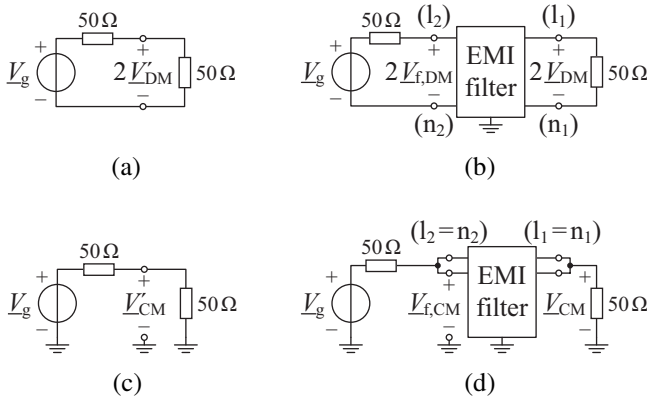

Fig. 6: Common measurement setups used to determine insertion losses of EMI filters with $50\,\Omega$ source and load resistors: (a), (b) measurements required to determine the DM insertion loss according to (8); (c), (d) measurements required to determine the CM insertion loss according to (9).

[4]The filter capacitor, C_b, is considered as part of the PFC rectifier in order to make the operation of the PFC rectifier without filter possible and to correctly interface to commercial EMI filters, which are often realized according to the filter circuit depicted in Fig. 11.

[5]Please note that the source voltages, $\underline{V}_{\text{s,DM}}$ and $\underline{V}_{\text{s,CM}}$, are not equal to the filter input voltages, $\underline{V}_{\text{f,DM}}$ and $\underline{V}_{\text{f,CM}}$, by reason of the filter input impedances $\underline{Z}_{\text{f,in,DM}}$ and $\underline{Z}_{\text{f,in,CM}}$, cf. Fig. 7.

received at the measurement ports of AMN 1 and AMN 2 to be processed by means of an accurate DM / CM-separator, cf. [21], in order to determine the DM and CM noise levels V'_{DM} and V'_{CM}. The subsequent calculations of the required DM and CM insertion losses include a factor two for both, $IL_{\mathrm{req,DM}}$ and $IL_{\mathrm{req,CM}}$, in order to comply with (10), i.e. to avoid that, *with* the EMI filter being used, $V_{\mathrm{DM}} + V_{\mathrm{CM}}$ exceeds V_{CISPR} at frequencies where V'_{DM} and V'_{CM} are approximately equal in magnitude:

$$IL_{\mathrm{req,DM}} = 2\frac{V'_{\mathrm{DM}}}{V_{\mathrm{CISPR}}}, \tag{11}$$

$$IL_{\mathrm{req,CM}} = 2\frac{V'_{\mathrm{CM}}}{V_{\mathrm{CISPR}}}, \tag{12}$$

$V'_{\mathrm{DM}}, V'_{\mathrm{CM}}$: DM and CM noise levels *without* EMI filter.

With known $IL_{\mathrm{req,DM}}$ and $IL_{\mathrm{req,CM}}$ it is theoretically possible to select a suitable EMI filter. This, however, is not directly possible, since manufacturers of EMI filters most commonly provide the insertion losses obtained with $50\,\Omega$ source and load impedances, $IL_{50,\mathrm{DM}}(f)$ and $IL_{50,\mathrm{CM}}(f)$. These insertion losses may considerably deviate from the actually achieved insertion losses, which is analyzed in the subsequent Section IV.

IV. Achieved insertion losses of the EMI filter

A. Achieved insertion loss

In a real application the PFC rectifier applies the generated EMI noise to its inner impedance and the input impedance of the EMI filter (Fig. 1 and **Fig. 7**). Thus, the voltage $\underline{V}_{\mathrm{f}}$ at the interface between the PFC rectifier and the EMI filter can be calculated according to:

$$\left.\frac{\underline{V}_{\mathrm{f}}}{\underline{V}_{\mathrm{s}}}\right|_{\underline{Z}_{\mathrm{o}}} = \left.\frac{\underline{Z}_{\mathrm{f,in}}}{\underline{Z}_{\mathrm{s}} + \underline{Z}_{\mathrm{f,in}}}\right|_{\underline{Z}_{\mathrm{o}}}. \tag{13}$$

The EMI filter attenuates $\underline{V}_{\mathrm{f}}$ according to the insertion loss $\underline{IL}_{0/\underline{Z}_{\mathrm{o}}}$, due to zero source impedance ($R \to 0$ in Fig. 7):

$$\left.\frac{\underline{V}_{\mathrm{f}}}{\underline{V}}\right|_{\underline{Z}_{\mathrm{o}}} = \underline{IL}_{0/\underline{Z}_{\mathrm{o}}}. \tag{14}$$

$\underline{IL}_{0/\underline{Z}_{\mathrm{o}}}$, thus, denotes a voltage attenuation and is equal to the reciprocal of the voltage transfer function of the filter, $\underline{IL}_{0/\underline{Z}_{\mathrm{o}}} = (\underline{V}/\underline{V}_{\mathrm{f}})^{-1}$. The input impedance, $\underline{Z}_{\mathrm{f,in}}$, and the voltage attenuation of the EMI filter depend on the termination impedance $\underline{Z}_{\mathrm{o}}$, which, in case of the AMN being connected, is approximately equal to $100\,\Omega$ for DM and $25\,\Omega$ for CM, cf. Section II.

Thus, the absolute value of the total voltage attenuation achieved with a particular EMI filter includes the interaction of filter and converter impedances and is given with:

$$\left.\frac{V_{\mathrm{s}}}{V}\right|_{\underline{Z}_{\mathrm{o}}} = \underbrace{\left|\frac{\underline{Z}_{\mathrm{s}} + \underline{Z}_{\mathrm{f,in}}}{\underline{Z}_{\mathrm{f,in}}}\right|_{\underline{Z}_{\mathrm{o}}}}_{\substack{\text{Multiplier due to the voltage}\\ \text{divider formed with } \underline{Z}_{\mathrm{s}} \text{ and } \underline{Z}_{\mathrm{f,in}}.}} \cdot \underbrace{IL_{0/\underline{Z}_{\mathrm{o}}}}_{\substack{\text{Voltage attenuation for a}\\ \text{given output impedance } \underline{Z}_{\mathrm{o}}.}}. \tag{15}$$

B. Differential Mode

In case of DM [Fig. 5(a) and (6)], expression (15) is:

$$\left.\frac{V_{\mathrm{s,DM}}}{V_{\mathrm{DM}}}\right|_{\underline{Z}_{\mathrm{o,DM}}} = \left.\frac{\underline{Z}_{\mathrm{s,DM}} + \underline{Z}_{\mathrm{f,in,DM}}}{\underline{Z}_{\mathrm{f,in,DM}}}\right|_{\underline{Z}_{\mathrm{o,DM}}} \cdot IL_{0/100,\mathrm{DM}}; \tag{16}$$

In order to evaluate the total DM insertion loss given with (16), two impedances and the voltage attenuation $IL_{0/100,\mathrm{DM}}$, which are detailed below, need to be known.

1) Input impedance of the filter, $\underline{Z}_{\mathrm{f,in,DM}}$: The DM input impedance of the EMI filter can be obtained by means of an impedance analyzer, measured with respect to magnitude and phase. The output of the filter is terminated with $100\,\Omega$, cf. Fig. 5(a).[6]

2) Inner impedance of the power converter, $\underline{Z}_{\mathrm{s,DM}}$: The depicted PFC rectifier employs a bridge rectifier and a boost converter. The bridge rectifier is operated with mains frequency and the conducting rectifier diodes show comparably low resistance values, so the input impedance of the bridge rectifier can be neglected in the considered frequency range. Thus, the DM input impedance of the PFC rectifier is approximately equal to the input impedance of the boost converter, $\underline{Z}_{\mathrm{boost}}$, which is analytically calculated from the small signal equivalent circuit derived in [23] and depicted in **Fig. 8**. The input impedance depends on the operating point and, for continuous conduction mode, is:

$$\underline{Z}_{\mathrm{boost}} = \underline{Z}_{C_{\mathrm{b}}} || \left[\underline{Z}_{L_{\mathrm{b}}} + D'^2 \cdot (\underline{Z}_C || R)\right], \tag{17}$$

[6] In practice, the input impedance $\underline{Z}_{\mathrm{f,in,DM}}$ may be measured for $\underline{Z}_{\mathrm{o,DM}} = 50\,\Omega$ or $\underline{Z}_{\mathrm{o,DM}} = 100\,\Omega$, since almost equal input impedances result in the stop band of the filter, cf. Fig. 14.

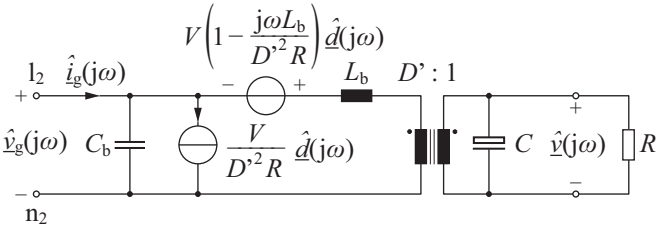

Fig. 8: Small signal equivalent circuit of a boost converter operated in continuous conduction mode [23]. The cut-off frequency of the current controller is typically considerably less than 150 kHz and, thus, $\hat{d}(\mathrm{j}\omega) \to 0$ applies in the considered frequency range. The impedance of the remaining network is given with (17).

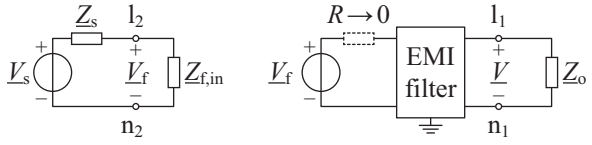

Fig. 7: The voltage applied to the EMI filter, $\underline{V}_{\mathrm{f}}$, depends on the source voltage $\underline{V}_{\mathrm{s}}$ and the impedances $\underline{Z}_{\mathrm{s}}$ and $\underline{Z}_{\mathrm{f,in}}$. The EMI filter attenuates $\underline{V}_{\mathrm{f}}$ according to the voltage attenuation $\underline{IL}_{0/\underline{Z}_{\mathrm{o}}}$.

whereupon D' denotes the duty cycle of the diode D and $\underline{Z}_C$ the impedance of the output DC capacitor.

The inner impedance $\underline{Z}_{\mathrm{s,DM}}$ can be measured according to [24] for a selection of different operating points. With this and (16), the actually achieved insertion loss can be evaluated for all considered operating points. In this work $\underline{Z}_{L_\mathrm{b}} \gg \underline{Z}_C||R$ is assumed and, due to $0 < D' < 1$, $\underline{Z}_{\mathrm{s,DM}} \approx \underline{Z}_{C_\mathrm{b}}||\underline{Z}_{L_\mathrm{b}}$ results, which is in accordance with (6) and [4] and can be measured with an impedance analyzer. **Fig. 9(a)** depicts the corresponding measurement setup: the diode D is removed, the MOSFET T is shorted, and the impedance $\underline{Z}_{\mathrm{s,DM}}$ is measured with an impedance analyzer connected to the l_2-n_2-port of the PFC rectifier.

3) Voltage attenuation of the filter, $IL_{0/100,\mathrm{DM}}$: $IL_{0/100,\mathrm{DM}}$ can be estimated from an already available insertion loss $IL_{50,\mathrm{DM}}$ that is obtained for $\underline{Z}_\mathrm{s} = \underline{Z}_\mathrm{o} = 50\,\Omega$ and, since filter manufacturers provide $IL_{50,\mathrm{DM}}$, the paper focuses on this estimation. Still, a direct measurement of $IL_{0/100,\mathrm{DM}}$ is feasible and will be briefly explained at the end of this subsection.

Regarding the measurement setup used to determine $IL_{50,\mathrm{DM}}$, the input voltage applied to the filter is related to the generator voltage according to:

$$\frac{2\underline{V}_{\mathrm{f,DM}}}{\underline{V}_\mathrm{g}} = \left.\frac{\underline{Z}_{\mathrm{f,in,DM}}}{50\,\Omega + \underline{Z}_{\mathrm{f,in,DM}}}\right|_{\underline{Z}_{\mathrm{o,DM}}=50\,\Omega} \quad \text{; cf. Fig. 6(b).} \tag{18}$$

The input voltage of the filter can be expressed in terms of the filter output voltage with the use of (8) and (18):

$$\begin{aligned} 2IL_{50,\mathrm{DM}} &= \left.\frac{V_\mathrm{g}}{2V_\mathrm{DM}}\right|_{\underline{Z}_{\mathrm{s,DM}}=\underline{Z}_{\mathrm{o,DM}}=50\,\Omega} \\ \rightarrow \quad \left.\frac{2V_{\mathrm{f,DM}}}{2V_\mathrm{DM}}\right|_{\underline{Z}_{\mathrm{o,DM}}=50\,\Omega} &= 2IL_{50,\mathrm{DM}} \left|\frac{\underline{Z}_{\mathrm{f,in,DM}}}{50\,\Omega + \underline{Z}_{\mathrm{f,in,DM}}}\right|_{\underline{Z}_{\mathrm{o,DM}}=50\,\Omega} \end{aligned} \tag{19}$$

The insertion loss $IL_{0/100,\mathrm{DM}}$ is calculated according to

$$IL_{0/100,\mathrm{DM}} = \left.\frac{V'_\mathrm{DM}}{V_\mathrm{DM}}\right|_{\underline{Z}_{\mathrm{s,DM}}=0,\underline{Z}_{\mathrm{o,DM}}=100\,\Omega} \tag{20}$$

whereupon $2V'_\mathrm{DM} = V_\mathrm{g} = 2V_{\mathrm{f,DM}}$ applies due to the zero source impedance:

$$IL_{0/100,\mathrm{DM}} = \frac{V_{\mathrm{f,DM}}}{V_\mathrm{DM}\big|_{\underline{Z}_{\mathrm{o,DM}}=100\,\Omega}}. \tag{21}$$

In order to express $IL_{0/100,\mathrm{DM}}$ in terms of $IL_{50,\mathrm{DM}}$, it is necessary to express the output voltage obtained for $\underline{Z}_{\mathrm{o,DM}} = 100\,\Omega$ in terms of the output voltage obtained for $\underline{Z}_{\mathrm{o,DM}} = 50\,\Omega$. The output voltage remains approximately equal for $\underline{Z}_{\mathrm{o,DM}} = 100\,\Omega$ and $\underline{Z}_{\mathrm{o,DM}} = 50\,\Omega$ if the last filter element is a parallel connected capacitor with sufficiently low impedance. If the last filter element that is connected in series to $\underline{Z}_{\mathrm{o,DM}}$ is an inductor with sufficiently large impedance, however, the current through $\underline{Z}_{\mathrm{o,DM}}$ remains approximately unchanged. With this, $V_\mathrm{DM}\big|_{\underline{Z}_{\mathrm{o,DM}}=100\,\Omega} = 2V_\mathrm{DM}\big|_{\underline{Z}_{\mathrm{o,DM}}=50\,\Omega}$ results. In summary, the resulting output voltage is:

$$V_\mathrm{DM}\big|_{\underline{Z}_{\mathrm{o,DM}}=100\,\Omega} \approx c_\mathrm{DM} V_\mathrm{DM}\big|_{\underline{Z}_{\mathrm{o,DM}}=50\,\Omega} \quad \text{with} \tag{22}$$

$$c_\mathrm{DM} = \begin{cases} \text{close to 1 for a mains-side DM filter capacitor,} \\ \text{close to 2 for a mains-side DM filter inductor.} \end{cases}$$

Thus, (19), (21), and (22) can be used to derive an expression for $IL_{0/100,\mathrm{DM}}$:

$$IL_{0/100,\mathrm{DM}} \approx \frac{2}{c_\mathrm{DM}} IL_{50,\mathrm{DM}} \left|\frac{\underline{Z}_{\mathrm{f,in,DM}}}{50\,\Omega + \underline{Z}_{\mathrm{f,in,DM}}}\right|_{\underline{Z}_{\mathrm{o,DM}}=50\,\Omega \text{ or } 100\,\Omega}. \tag{23}$$

The input impedance $\underline{Z}_{\mathrm{f,in,DM}}$ may be measured for $\underline{Z}_{\mathrm{o,DM}} = 50\,\Omega$ or $\underline{Z}_{\mathrm{o,DM}} = 100\,\Omega$, since almost equal input impedances result in the stop band of the filter, cf. Fig. 14.

It is also possible to directly determine the voltage attenuation based on the measurement setup depicted in **Fig. 10(a)**, which is similar to the measurement setup shown in [9], [10]. This setup employs conventional $50\,\Omega$ equipment, features a low-impedance voltage source (approximately $0.1\,\Omega$ up to high frequencies), and enables the measurement of $IL_{0.1/100,\mathrm{DM}}$. The voltage attenuations introduced by the 7:1 transformer and

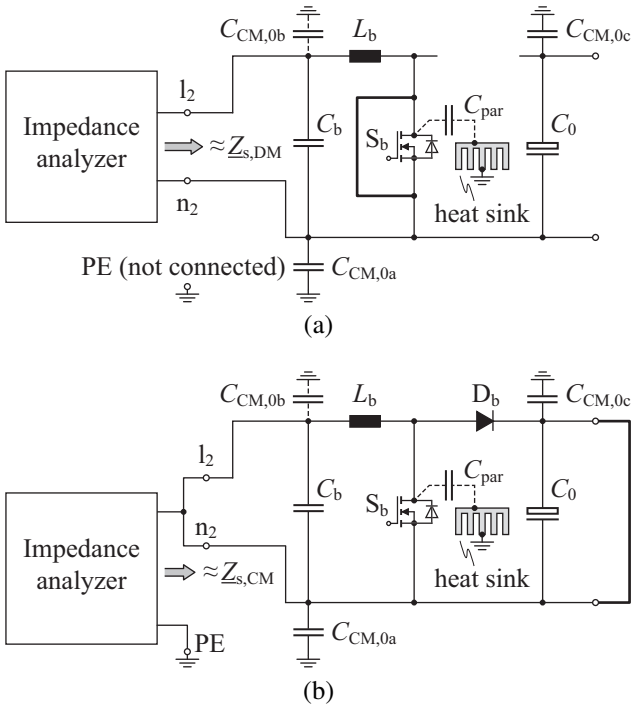

Fig. 9: Measurement setups used to determine (a) $\underline{Z}_{\mathrm{s,DM}}$ and (b) $\underline{Z}_{\mathrm{s,CM}}$. The earth capacitances $C_{\mathrm{CM,0a}}$, $C_{\mathrm{CM,0b}}$, and $C_{\mathrm{CM,0c}}$ result from parasitic capacitances and / or actually placed capacitors. In the considered example setup $C_{\mathrm{CM,0b}} = C_{\mathrm{CM,0c}} = 15\,\mathrm{nF}$ are actually placed, $C_{\mathrm{CM,0a}}$ is parasitic only. The total capacitance, $C_{\mathrm{CM,0}}$ depicted in Fig. 5(b), is the sum of $C_{\mathrm{CM,0a}}$, $C_{\mathrm{CM,0b}}$, and $C_{\mathrm{CM,0c}}$, cf. [6].

the resistive dividers are approximately $49\,\mathrm{dB}$. For $Z_{\mathrm{f,in,DM}} \gg 0.1\,\Omega$, the insertion loss $IL_{0.1/100,\mathrm{DM}}$ is an estimate of the voltage attenuation $IL_{0/100,\mathrm{DM}}$:

$$IL_{0/100,\mathrm{DM}} \approx IL_{0.1/100,\mathrm{DM}} \approx \approx \frac{V_\mathrm{g}}{2V_\mathrm{m,DM}} 10^{\frac{-49\,\mathrm{dB}}{20}} \quad \forall \quad Z_{\mathrm{f,in,DM}} \gg 0.1\,\Omega. \quad (24)$$

C. Common Mode

The expressions for the achieved DM and CM insertion losses are very similar but not identical. Therefore, this Section briefly summarizes the results obtained for CM. The absolute value of the total CM insertion loss achieved with a particular EMI filter is:

$$\left.\frac{V_\mathrm{s,CM}}{V_\mathrm{CM}}\right|_{\underline{Z}_\mathrm{o,CM}} = \left.\left|\frac{\underline{Z}_\mathrm{s,CM}+\underline{Z}_\mathrm{f,in,CM}}{\underline{Z}_\mathrm{f,in,CM}}\right|\right|_{\underline{Z}_\mathrm{o,CM}} \cdot IL_{0/25,\mathrm{CM}}. \quad (25)$$

1) Impedances $\underline{Z}_\mathrm{f,in,CM}$ and $\underline{Z}_\mathrm{s,CM}$: The CM input impedance of the EMI filter can be measured with an impedance analyzer, whereas the output of the filter is terminated with a $25\,\Omega$ resistor, cf. Fig. 5(b).[7]

The CM impedance of the PFC rectifier, derived according to [6], essentially consists of two capacitors, C_par and $C_\mathrm{CM,0}$, depicted in Fig. 5(b). The capacitance C_par denotes the parasitic capacitance formed by the back side of the MOSFET, the thermal interface pad, and the earthed heat sink. The remaining capacitor, $C_\mathrm{CM,0}$, is the sum of all remaining capacitances to earth [6].

The CM impedance depends on the operating point and may be measured according to [25]. In this work, the total CM converter impedance, $\underline{Z}_\mathrm{s,CM} \approx \underline{Z}_{C_\mathrm{par}} || \underline{Z}_{C_\mathrm{CM,0}}$, is obtained from an impedance measurement using the measurement setup depicted in **Fig. 9(b)**. The impedance of the capacitance C_par, $\underline{Z}_{C_\mathrm{par}}$, is separately measured and $\underline{Z}_{C_\mathrm{CM,0}}$ is estimated from $\underline{Z}_\mathrm{s,CM}$ and $\underline{Z}_{C_\mathrm{par}}$ according to:

$$\frac{1}{\underline{Z}_{C_\mathrm{CM,0}}} = \frac{1}{\underline{Z}_\mathrm{s,CM}} - \frac{1}{\underline{Z}_{C_\mathrm{par}}}. \quad (26)$$

2) Voltage attenuation of the filter, $IL_{0/25,\mathrm{CM}}$: Similar to the derivations presented for DM, it is possible to determine $IL_{0/25,\mathrm{CM}}$ from an already available insertion loss measurement with $\underline{Z}_\mathrm{s} = \underline{Z}_\mathrm{o} = 50\,\Omega$, cf. Fig. 6(d):

$$IL_{0/25,\mathrm{CM}} \approx \frac{2}{c_\mathrm{CM}} IL_{50,\mathrm{CM}} \left.\left|\frac{\underline{Z}_\mathrm{f,in,CM}}{50\,\Omega+\underline{Z}_\mathrm{f,in,CM}}\right|\right|_{\underline{Z}_\mathrm{o,CM}=50\,\Omega \text{ or } 25\,\Omega}. \quad (27)$$

The factor c_CM,

$$c_\mathrm{CM} = \begin{cases} \text{close to 1/2 for a mains-side CM filter inductor,} \\ \text{close to 1 for a mains-side CM filter capacitor,} \end{cases} \quad (28)$$

results due to the interaction of $\underline{Z}_\mathrm{o,CM}$ and the mains-side filter impedance, cf. (22).

$IL_{0/25,\mathrm{CM}}$ can also be approximately measured with the setup depicted in **Fig. 10(b)**. Here, the attenuation introduced by the 7:1 transformer and the resistive divider is $43\,\mathrm{dB}$. This is $6\,\mathrm{dB}$ less attenuation compared to the DM measurement, since no resistive voltage divider is needed at the output side; cf. Fig. 10(a).

D. Discussion and summary

According to the investigations presented above, not only the insertion losses (or the voltage attenuations) but also the input impedances of the EMI filter need to be known in order to enable meaningful predictions of the achieved DM and CM insertion losses. Furthermore, the inner impedances of the considered power converter, $\underline{Z}_\mathrm{s,DM}$ and $\underline{Z}_\mathrm{s,CM}$, need to be determined. With this, (16), (25), and measured (or simulated) DM and CM noise levels that result if the PFC rectifier is operated without EMI filter,

$$V'_\mathrm{DM}(f) = V_\mathrm{s,DM}(f) \left|\frac{100\,\Omega}{100\,\Omega+\underline{Z}_\mathrm{s,DM}}\right|, \quad (29)$$

$$V'_\mathrm{CM}(f) = V_\mathrm{s,CM}(f) \left|\frac{25\,\Omega}{25\,\Omega+\underline{Z}_\mathrm{s,CM}}\right|, \quad (30)$$

the realized DM and CM insertion losses of the EMI filter,

$$IL_\mathrm{DM} = \frac{V'_\mathrm{DM}}{V_\mathrm{DM}} \quad \text{and} \quad IL_\mathrm{CM} = \frac{V'_\mathrm{CM}}{V_\mathrm{CM}}, \quad (31)$$

can be predicted:

$$IL_\mathrm{DM} = IL_{0/100,\mathrm{DM}} \left|\frac{100\,\Omega}{100\,\Omega+\underline{Z}_\mathrm{s,DM}} \cdot \frac{\underline{Z}_\mathrm{s,DM}+\underline{Z}_\mathrm{f,in,DM}}{\underline{Z}_\mathrm{f,in,DM}}\right|, \quad (32)$$

$$IL_\mathrm{CM} = IL_{0/25,\mathrm{CM}} \left|\frac{25\,\Omega}{25\,\Omega+\underline{Z}_\mathrm{s,CM}} \cdot \frac{\underline{Z}_\mathrm{s,CM}+\underline{Z}_\mathrm{f,in,CM}}{\underline{Z}_\mathrm{f,in,CM}}\right|. \quad (33)$$

[7] In practice, the input impedance $\underline{Z}_\mathrm{f,in,CM}$ may be measured for $\underline{Z}_\mathrm{o,CM} = 50\,\Omega$ or $\underline{Z}_\mathrm{o,CM} = 25\,\Omega$, since almost equal input impedances result in the stop band of the filter.

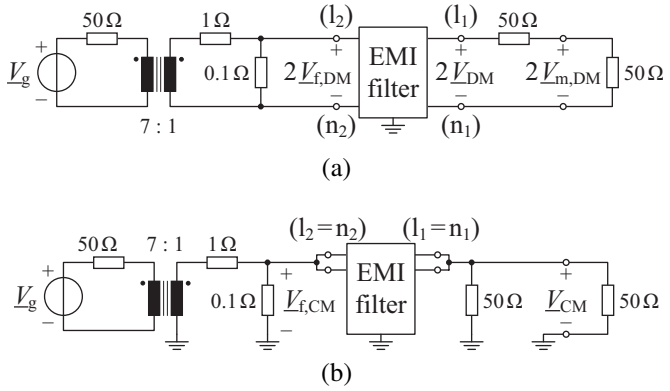

Fig. 10: Proposed measurement setups used to determine (a) $IL_{0.1/100,\mathrm{DM}}$ and (b) $IL_{0.1/25,\mathrm{CM}}$, cf. (24). The input impedances of approximately $0.1\,\Omega$ are selected according to [9]. The output impedances of $100\,\Omega$ (DM) or $25\,\Omega$ (CM) are selected based on the DM / CM impedances of the AMNs connected to the EMI filter.

Thus, the results obtained in this Section facilitate the calculation of IL_{DM} and IL_{CM} based on the commonly documented insertion losses $IL_{50,\mathrm{DM}}$ and $IL_{50,\mathrm{CM}}$ according to:

$$IL_{\mathrm{DM}} = \frac{IL_{\mathrm{DM}}}{IL_{0/100,\mathrm{DM}}} \frac{IL_{0/100,\mathrm{DM}}}{IL_{50,\mathrm{DM}}} IL_{50,\mathrm{DM}}, \tag{34}$$

$$IL_{\mathrm{CM}} = \frac{IL_{\mathrm{CM}}}{IL_{0/25,\mathrm{CM}}} \frac{IL_{0/25,\mathrm{CM}}}{IL_{50,\mathrm{CM}}} IL_{50,\mathrm{CM}}, \tag{35}$$

with

$$\frac{IL_{\mathrm{DM}}}{IL_{0/100,\mathrm{DM}}} = \left| \frac{100\,\Omega}{100\,\Omega + \underline{Z}_{\mathrm{s,DM}}} \cdot \frac{\underline{Z}_{\mathrm{s,DM}} + \underline{Z}_{\mathrm{f,in,DM}}}{\underline{Z}_{\mathrm{f,in,DM}}} \right|, \tag{36}$$

$$\frac{IL_{0/100,\mathrm{DM}}}{IL_{50,\mathrm{DM}}} \approx \frac{2}{c_{\mathrm{DM}}} \left| \frac{\underline{Z}_{\mathrm{f,in,DM}}}{50\,\Omega + \underline{Z}_{\mathrm{f,in,DM}}} \right|, \tag{37}$$

$$\frac{IL_{\mathrm{CM}}}{IL_{0/25,\mathrm{CM}}} = \left| \frac{25\,\Omega}{25\,\Omega + \underline{Z}_{\mathrm{s,CM}}} \cdot \frac{\underline{Z}_{\mathrm{s,CM}} + \underline{Z}_{\mathrm{f,in,CM}}}{\underline{Z}_{\mathrm{f,in,CM}}} \right|, \tag{38}$$

$$\frac{IL_{0/25,\mathrm{CM}}}{IL_{50,\mathrm{CM}}} \approx \frac{2}{c_{\mathrm{CM}}} \left| \frac{\underline{Z}_{\mathrm{f,in,CM}}}{50\,\Omega + \underline{Z}_{\mathrm{f,in,CM}}} \right|. \tag{39}$$

The EMI requirements are fulfilled if the DM and CM insertion losses achieved with the selected EMI filter are greater than $IL_{\mathrm{req,DM}}$ and $IL_{\mathrm{req,CM}}$ defined with (11) and (12):[8]

$$IL_{\mathrm{DM}} > IL_{\mathrm{req,DM}}, \tag{40}$$

$$IL_{\mathrm{CM}} > IL_{\mathrm{req,CM}}. \tag{41}$$

V. Experimental results

Fig. 11 depicts the EMI filter network and shows the component values used for the investigated PFC rectifier. According to Section III, conducted DM and CM noise are first determined without EMI filter in order to facilitate the calculations of the required insertion losses. In a second step the actually achieved insertion losses (DM and CM) are determined and the noise spectrum that results with the considered EMI filter is calculated.

[8]Expressions (40) and (41) are sufficient and not necessary criterias, i.e. either (40) or (41) may be violated if the sum of the emitted CM and DM noise does not exceed the limit defined in the CISPR regulation.

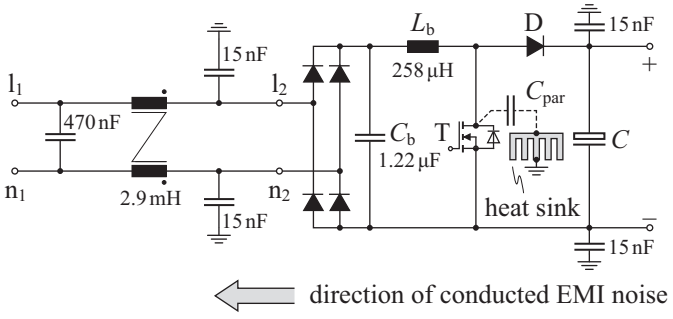

Fig. 11: Schematic drawing of the filter network and component values used in the investigated PFC rectifier. Here, $c_{\mathrm{DM}} = 1$ and $c_{\mathrm{CM}} = 1/2$ applies, cf. (22) and (28).

A. DM and CM noise without EMI filter

Fig. 12 depicts the DM and CM spectra calculated for operation without EMI filter. This calculation uses (5) – (7) and the noise models of Fig. 5. The impedances $\underline{Z}_{L_{\mathrm{b}}}$, $\underline{Z}_{C_{\mathrm{b}}}$, $\underline{Z}_{C_{\mathrm{par}}}$, and $\underline{Z}_{C_{\mathrm{CM,0}}}$ are obtained from measurements. The required insertion losses $IL_{\mathrm{req,DM}}$ and $IL_{\mathrm{req,CM}}$ are directly given by the distances between $V'_{\mathrm{DM}}(nf_{\mathrm{s}})$ and $V'_{\mathrm{CM}}(nf_{\mathrm{s}})$ to the respective noise limits depicted in Fig. 12.

B. Predicted insertion loss of the EMI filter

Expressions (34) – (39) facilitate the prediction of the actually realized insertion losses based on the insertion losses measured for $\underline{Z}_{\mathrm{s}} = \underline{Z}_{\mathrm{o}} = 50\,\Omega$. For this, the DM and CM input impedances of the EMI filter and the input impedances of the PFC rectifier are measured according to Section IV (**Fig. 13** and **Fig. 14** depict the DM impedances $\underline{Z}_{\mathrm{s,DM}}$ and $\underline{Z}_{\mathrm{f,in,DM}}$).

Fig. 15 shows the insertion losses measured for $\underline{Z}_{\mathrm{s}} = \underline{Z}_{\mathrm{o}} = 50\,\Omega$ and the estimated insertion losses $IL_{0/100,\mathrm{DM}}$, IL_{DM}, $IL_{0/25,\mathrm{CM}}$, and IL_{CM}. The multipliers needed to calculate the

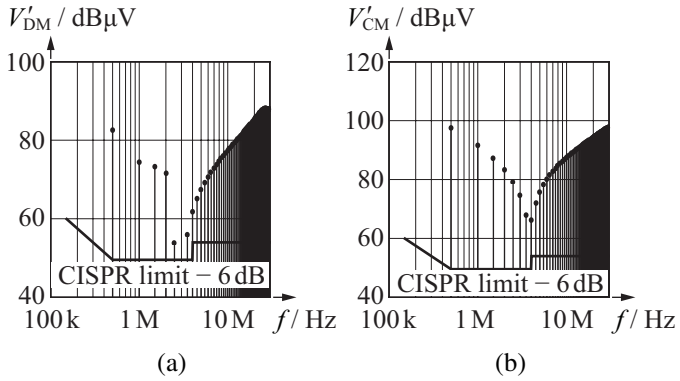

Fig. 12: Calculated DM and CM noise spectra if no EMI filter is used: (a) DM, (b) CM. The distances of each spectral component to the depicted limits give the required insertion losses $IL_{\mathrm{req,DM}}$ and $IL_{\mathrm{req,CM}}$.

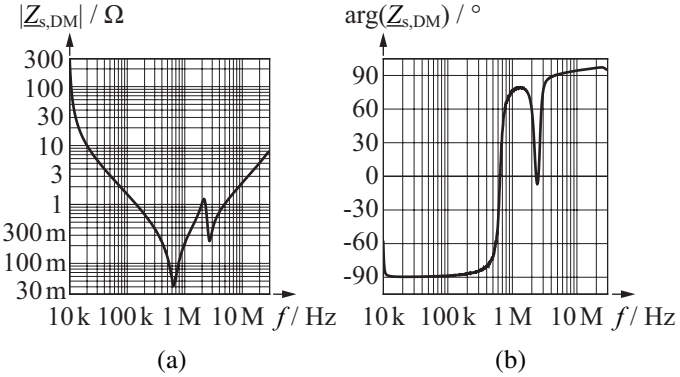

Fig. 13: Measured DM input impedance of the PFC rectifier, $\underline{Z}_{\mathrm{s,DM}}$: (a) absolute value, (b) phase angle.

estimated insertion losses, depicted in **Fig. 16**, are obtained from (36) – (39) for the measured impedances. It can be seen that the multipliers $IL_{0/100,\mathrm{DM}}/IL_{50,\mathrm{DM}}$ and $IL_{0/25,\mathrm{CM}}/IL_{50,\mathrm{CM}}$ contribute most to the total multipliers $IL_{\mathrm{DM}}/IL_{50,\mathrm{DM}}$ and $IL_{\mathrm{CM}}/IL_{50,\mathrm{CM}}$, i.e. $IL_{0/100,\mathrm{DM}}$ and $IL_{0/25,\mathrm{CM}}$, which are close to the approximate worst case insertion loss defined in [10], may serve as indicators for the finally realized insertion losses. Still, interactions at the interface between PFC rectifier and EMI filter additionally modify the actual insertion losses and

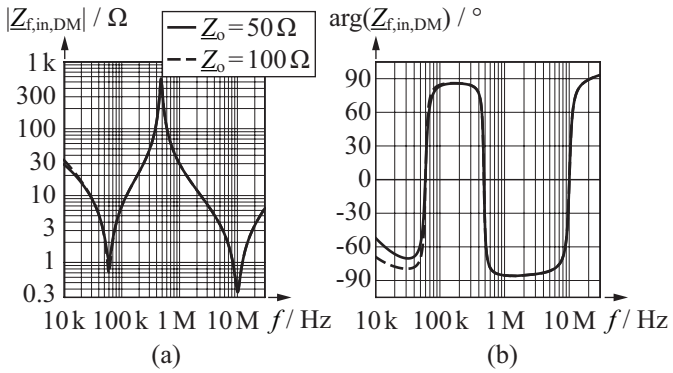

Fig. 14: Measured DM impedance of the EMI filter, $\underline{Z}_{\mathrm{f,in,DM}}$, measured according to Fig. 9(a): (a) absolute value, (b) phase angle.

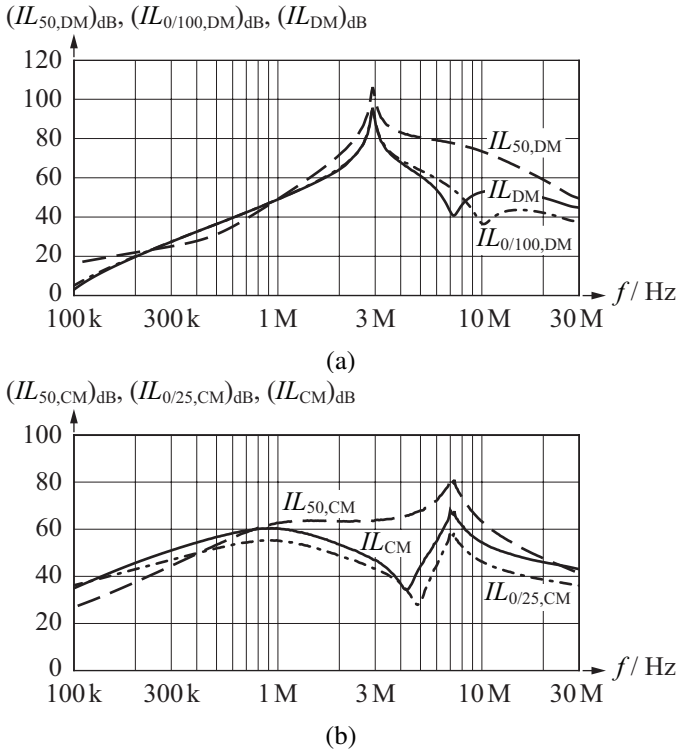

Fig. 15: Measured insertion losses ($IL_{50,\mathrm{DM}}$, $IL_{50,\mathrm{CM}}$) and estimated insertion losses ($IL_{0/100,\mathrm{DM}}$, $IL_{0/25,\mathrm{CM}}$, IL_{DM}, and IL_{CM}) for (a) DM and (b) CM.

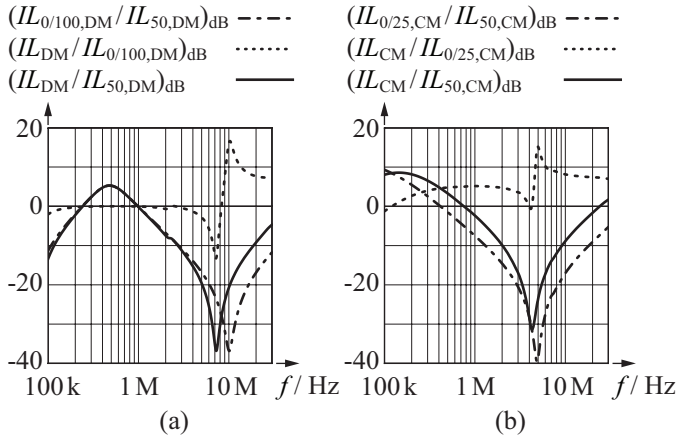

Fig. 16: (a) DM multipliers $IL_{0/100,\mathrm{DM}}/IL_{50,\mathrm{DM}}$, $IL_{\mathrm{DM}}/IL_{0/100,\mathrm{DM}}$, and $IL_{\mathrm{DM}}/IL_{50,\mathrm{DM}}$; (b) CM multipliers $IL_{0/100,\mathrm{CM}}/IL_{50,\mathrm{CM}}$, $IL_{\mathrm{CM}}/IL_{0/100,\mathrm{CM}}$, and $IL_{\mathrm{CM}}/IL_{50,\mathrm{CM}}$. The insertion losses of the considered EMI filter are mainly reduced by $IL_{0/100}/IL_{50}$ (DM and CM). Still, interactions at the interface between PFC rectifier and EMI filter have an additional impact on the expected insertion losses.

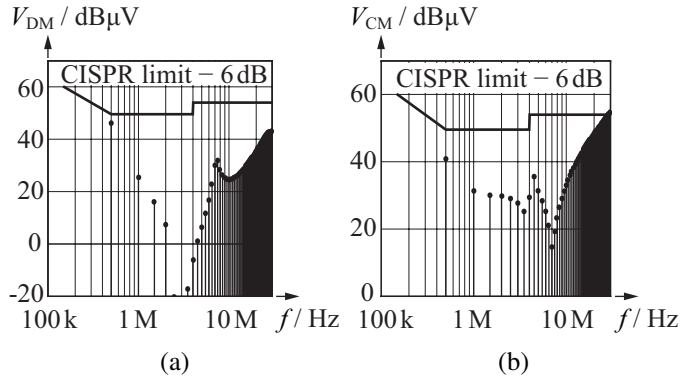

Fig. 17: (a) Predicted DM noise and (b) predicted CM noise with EMI filter being used.

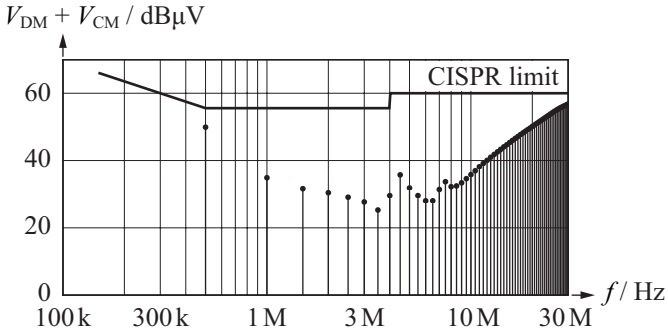

Fig. 18: Sum of the predicted DM and CM spectral noise components, $V_{\mathrm{DM}} + V_{\mathrm{CM}}$. According to this result the considered EMI filter is expected to fulfill the requirements of [10].

may yield insertion losses that are less than the approximate worst-case insertion losses of [10], e.g. for $4\,\mathrm{MHz} < f < 8\,\mathrm{MHz}$ in Fig. 16(a).

The DM and CM spectral noise components with EMI filter, estimated with the predicted insertion losses IL_{DM} and IL_{CM}, are depicted in **Fig. 17**. The sum of DM and CM noise components, $V_{\mathrm{DM}}(nf_{\mathrm{s}})+V_{\mathrm{CM}}(nf_{\mathrm{s}})$, is shown in **Fig. 18**. According to this result and due to (10) the considered EMI filter is expected to fulfill the requirements.

VI. Conclusion

This paper details a method to predict DM and CM insertion losses of an EMI filter based on already available insertion losses $IL_{50,\mathrm{DM}}$ and $IL_{50,\mathrm{CM}}$, i.e. insertion losses measured with a generator with $50\,\Omega$ source impedance and a test receiver with $50\,\Omega$ input impedance. Based on an example PFC rectifier it is shown that the impedances at the interface between the EMI filter and the PFC rectifier considerably modify the realized insertion losses. Thus, besides $IL_{50,\mathrm{DM}}$ and $IL_{50,\mathrm{CM}}$, the frequency behaviors of the four impedances listed below need to be known in order to facilitate a prediction of the achieved insertion losses.

- The filter's DM and CM input impedances with respect to amplitude and phase, $\underline{Z}_{\mathrm{f,in,DM}}$ and $\underline{Z}_{\mathrm{f,in,CM}}$, if the filter is terminated with $50\,\Omega$. These impedances can be provided by the manufacturer of the EMI filter.
- The DM and CM source impedances of the converter with respect to amplitude and phase, $\underline{Z}_{\mathrm{s,DM}}$ and $\underline{Z}_{\mathrm{s,CM}}$, which need to be determined by the manufacturer of the power converter.

Acknowledgement

The authors are very grateful to Mr. S. Pasko and Mr. N. Häberle, both of Schaffner EMV AG, for valuable advices and suggestions.

References

[1] *CISPR11: Industrial, scientific and medical equipment - Radio-frequency disturbance characteristics - Limits and methods of measurement*, International Electrotechnical Commission (IEC) Std.

[2] *CISPR16: Specification for radio disturbance and immunity measuring apparatus and methods*, International Electrotechnical Commission (IEC) Std.

[3] M. L. Heldwein, "EMC filtering of three-phase PWM converters," Ph.D. dissertation, ETH Zurich, 2008.

[4] K. Raggl, T. Nussbaumer, and J. W. Kolar, "Guideline for a simplified differential-mode EMI filter design," *IEEE Transactions on Industrial Electronics*, vol. 57, no. 3, pp. 1031–1040, 2010.

[5] V. Tarateeraseth, K. Y. See, F. G. Canavero, and R. W. Chang, "Systematic electromagnetic interference filter design based on information from in-circuit impedance measurements," *IEEE Transactions on Electromagnetic Compatibility*, vol. 52, no. 3, pp. 588 – 598, 2010.

[6] H. Ye, Z. Yang, J. Dai, C. Yan, X. Xin, and J. Ying, "Common mode noise modeling and analysis of dual boost PFC circuit," in *Proc. of the 26th Annual International Telecommunications Energy Conference (INTELEC)*, 2004, pp. 575 – 582.

[7] J. R. Nicholson and J. A. Malack, "RF impedance of power lines and line impedance stabilization networks in conducted interference measurements," *IEEE Transactions on Electromagnetic Compatibility*, vol. EMC-15, no. 2, pp. 84 – 86, 1973.

[8] J. A. Malack and J. R. Engstrom, "RF impedance of united states and european power lines," *IEEE Transactions on Electromagnetic Compatibility*, vol. EMC-18, no. 1, pp. 36 – 38, 1976.

[9] H. M. Schlicke, "Assuredly effective filters," *IEEE Transactions on Electromagnetic Compatibility*, vol. EMC-18, no. 3, pp. 106–110, 1976.

[10] *CISPR17: Methods of measurement of the suppression characteristics of passive EMC filtering devices*, International Electrotechnical Commission (IEC) Std.

[11] B. Audone and L. Bolla, "Insertion loss of mismatched EMI suppressors," *IEEE Transactions on Electromagnetic Compatibility*, vol. EMC-20, no. 3, pp. 384 – 389, 1978.

[12] F. Broyde and E. Clavelier, "Minimum attenuation and input impedance domain of a linear filter," in *Proc. of the 8th International Zurich Symposium on Electromagnetic Compatibility*, Mar. 1989, pp. 261–266.

[13] *IEEE Std 1560-2005: IEEE Standard for Methods of Measurement of Radio Frequency Power Line Interference Filter in the Range of 100 Hz to 10 GHz*, Institute of Electrical and Electronics Engineers (IEEE) Std., 2006.

[14] A. Perez, A.-M. Sanchez, J.-R. Regue, M. Ribo, P. Rodriguez-Cepeda, and F.-J. Pajares, "Characterization of power-line filters and electronic equipment for prediction of conducted emissions," *IEEE Transactions on Electromagnetic Compatibility*, vol. 50, no. 3, pp. 577 – 585, 2008.

[15] J. Drinovsky, Z. Kejik, V. Ruzek, and J. Zachar, "EMI filters worst-case identification by alternative measurement system," *International Journal of Circuits Systems and Signal Processing*, vol. 5, no. 3, pp. 212–219, 2011.

[16] H. Rebholz and S. Tenbohlen, "Prospects and limits of common- and differential-mode separation for the filter development process," in *International Symposium on Electromagnetic Compatibility - EMC Europe*, 2008, pp. 1 – 6.

[17] S. M. Vakil, "A technique for determination of filter insertion loss as a function of arbitrary generator and load impedances," *IEEE Transactions on Electromagnetic Compatibility*, vol. EMC-20, no. 2, pp. 273 – 278, 1978.

[18] J. Svacina, Z. Kejik, V. Ruzek, J. Zachar, and J. Drinovsky, "EMI mains filter insertion loss estimation impedance termination unmatched impedance system," *Radioengineering*, vol. 20, no. 1, pp. 295–298, Apr. 2011.

[19] F. Broyde and E. Clavelier, "Designing power-line filter for their worst-case behaviour," in *Proc. of the 9th International Zurich Symposium on Electromagnetic Compatibility*, Mar. 1991, pp. 583–588.

[20] K. Y. See, "Network for conducted EMI diagnosis," *Electronics Letters*, vol. 35, no. 17, pp. 1446 – 1447, 1999.

[21] S. Wang, F. C. Lee, and W. G. Odendaal, "Characterization, evaluation, and design of noise separator for conducted emi noise diagnosis," *IEEE Transactions on Power Electronics*, vol. 20, no. 4, pp. 974 – 982, 2005.

[22] H. Bishnoi, A. C. Baisden, P. Mattavelli, and D. Boroyevich, "Analysis of EMI terminal modeling of switched power converters," *IEEE Transactions on Power Electronics*, vol. 27, no. 9, pp. 3924 – 3933, 2012.

[23] R. W. Erickson and D. Maksimovic, *Fundamentals of Power Electronics*, 2nd ed. Springer, 2001.

[24] Y. Panov and M. Jovanovic, "Practical issues of input/output impedance measurements in switching power supplies and application of measured data to stability analysis," in *Proc. of the 20th Annual IEEE Applied Power Electronics Conference and Exposition (APEC)*, vol. 2, 2005, pp. 1339 – 1345.

[25] K. Y. See and J. Deng, "Measurement of noise source impedance of SMPS using a two probes approach," *IEEE Transactions on Power Electronics*, vol. 19, no. 3, pp. 862 – 868, 2004.